

MOAC – A HIGH ACCURACY CALORIMETER FOR COLD FUSION STUDIES

SCOTT R. LITTLE, GEORGE A. LUCE, MARISSA E. LITTLE

*EarthTech International, Inc., 11855 Research Blvd
Austin, TX 78759, USA*

Calorimetry is conceptually simple but considerable effort is required to reduce systematic errors to acceptable levels. Since 1989, we have designed and constructed a dozen calorimeter systems for cold fusion research. Each of these systems provided valuable experience in error detection and correction. The culmination of our efforts, an instrument with a design accuracy of 0.1% relative, is nicknamed MOAC (Mother Of All Calorimeters). This paper provides a description of MOAC and presents some pertinent calorimetric results.

1. Introduction

One of the most important effects associated with cold fusion is excess heat. In order to measure excess heat a special calorimeter is required; one that simultaneously measures both the electrical power into the cell and the heat power out of the cell. Most of the calorimeters routinely used in chemical studies are unsuitable for this purpose because they only measure the heat power or energy released by the specimen.

For cold fusion research it is desirable to have a calorimeter with high accuracy so that small effects can be studied. Unfortunately, high-accuracy calorimetry is not easily achieved. It is especially difficult to realize accuracy better than 1% relative. Compared to a calorimeter with 1% accuracy, at least an order of magnitude more effort is required to achieve 0.1% accuracy^a.

MOAC was designed and constructed over an 8-month period from November 2003 to June 2004. Having constructed and tested a number of other calorimeters in the preceding 15 years, we were able to draw from a wide and varied experience in the design of MOAC. This experience was surely beneficial but, as you will see below, MOAC presented its own unique set of challenging systematic errors that had to be identified and eliminated before its performance would begin to approach the design accuracy goal of +/- 0.1% relative.

2. Measurement Strategy

MOAC operates on a simple principle. Flowing water is used to extract the heat from the cell. The flow rate and the temperature rise of the water are measured. The product of the temperature rise, the flow rate, and the specific heat of water yields the heat power being extracted from the cell. This approach is commonly referred to as flow calorimetry. In addition, MOAC simultaneously measures the heat output of the cell by isoperibolic calorimetry. In this technique, which is based upon Newton's Law of Cooling, the heat output power is assumed to be proportional to the temperature difference between the electrolyte and the gently stirred air that surrounds the cell. These two independent methods of heat power measurement provide important insights into the thermal behavior of cold fusion cells.

The cell is placed in an insulated chamber with a liquid-air heat exchanger and a small fan. This stirred-air environment provides relatively weak thermal coupling to the calorimetry water, which allows the cell to operate at elevated temperatures if desired.

^a McCullough & Scott, "Experimental Thermodynamics, Calorimetry of non-reacting systems", D.W. Butterworth, London, p.9, Vol. 1, 1968,

3. Construction

3.1. Overview

Despite its simple concept, MOAC is not a simple instrument. Two independent computer-based data acquisition systems monitor a total of forty-five parameters, including twenty-two separate temperatures. Fourteen analog outputs, driven by proportional-derivative feedback algorithms, control various critical parameters. Figure 1 shows a simplified block diagram of the system.

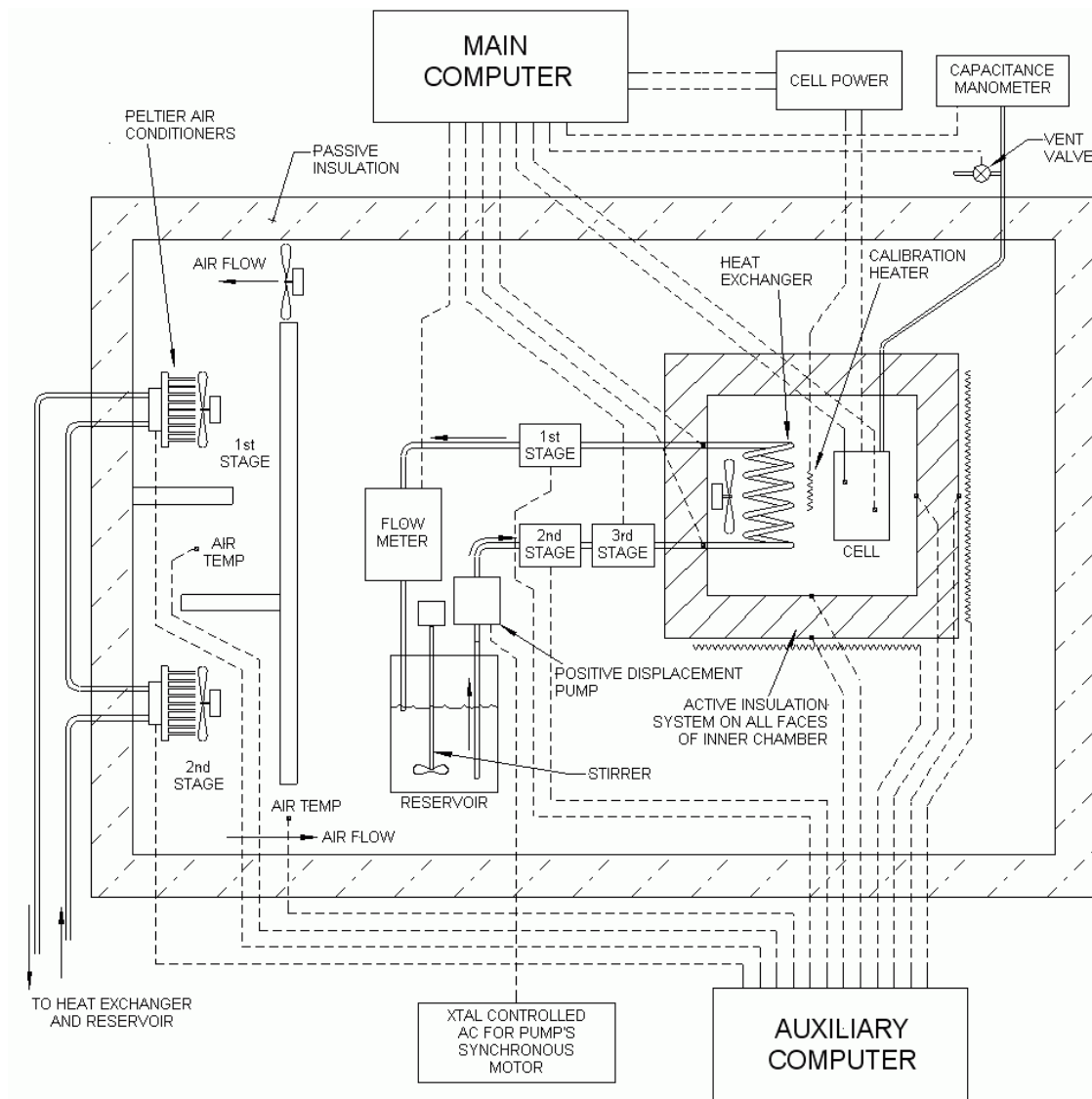


Figure 1. Block Diagram of MOAC

The cold fusion cell, heat exchanger, fan, and permanent calibration heater are located in the calorimetry chamber (CC) whose walls are made almost perfectly insulating by a system that heats the outer surface of each of the six wall panels so that its temperature matches that of the corresponding inner surface. This active insulation (AI) ensures that virtually all of the heat dissipated by the cell leaves the chamber via the flowing water.

A three-stage Peltier temperature regulator (which can add or remove heat as needed) controls the temperature of the water entering the heat exchanger. A positive-displacement pump driven by a synchronous motor powered by a crystal-based oscillator produces a stable flow of about 2.5 gm/s. This flow rate gives MOAC a nominal sensitivity of about 10 W/°C. A flowmeter consisting of an automated batch weighing system measures the flow rate periodically. A large insulated environmental enclosure (EE) houses the entire system. Air circulates over the calorimetry apparatus and then is ducted to a two-stage Peltier air conditioner where its temperature is tightly regulated before it re-enters the enclosure.

Figure 2 is a photograph of the entire system. The CC is the light blue box visible inside the wooden environmental enclosure. Also visible through the door window is the water reservoir and the flowmeter. Under the computer bench is a bank of DC power supplies. Under the bench that supports the EE is the water reservoir and heat exchanger for the Peltier air conditioners.



Figure 2. Overall View of MOAC

Error! Not a valid bookmark self-reference. is a photograph of the workspace of the EE. On the left is the flowmeter and water reservoir (gallon jug). On the far left at the bottom is the positive-displacement pump. On the right is the CC. In the foreground at the bottom are the terminal strips that provide all electrical connections to the interior of the CC.

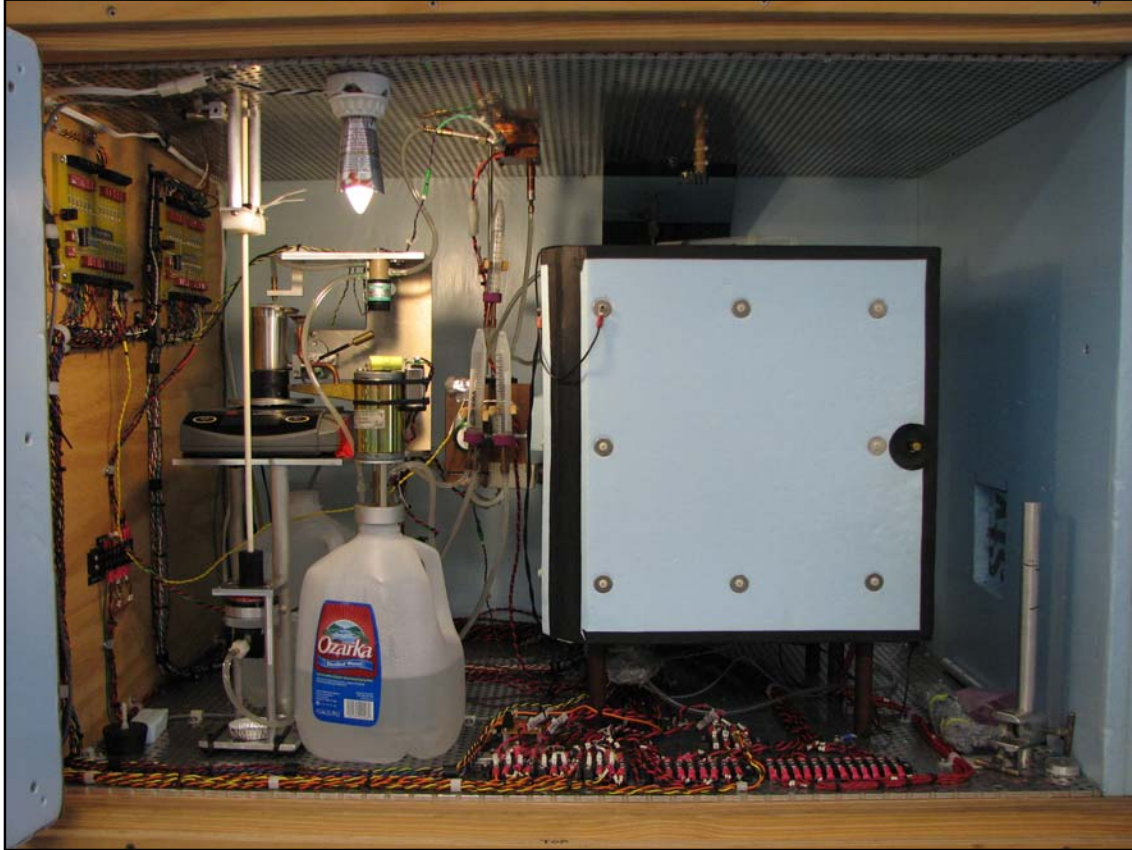


Figure 3. Workspace of Environmental Enclosure

Figure 4 is a photograph of the interior of the CC. On the right is the cell, in this case our standard calibration cell. On the left is the liquid-air heat exchanger and fan. Between the heat exchanger and the cell is the permanent calibration heater. In the foreground at the bottom is a liquid trap that collects any liquid ejected from the cell and protects the pressure measurement sensor located outside the enclosures.

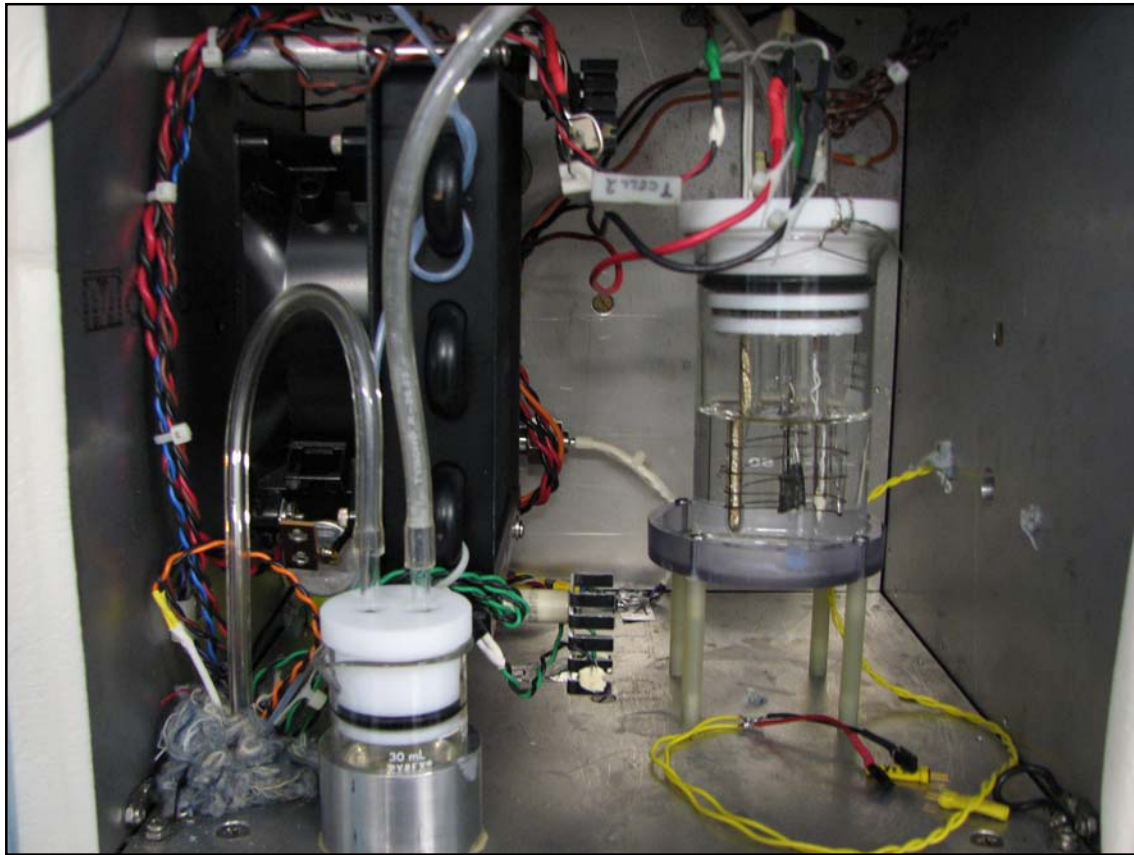


Figure 4. Calorimetry Chamber

3.2. Environmental Enclosure (EE)

The EE is the temperature-controlled housing for the water flow system and the CC. The EE is a 19 mm thick plywood shell lined with two layers of 19 mm thick rigid polystyrene foam insulation^b that has a thermal conductivity of 0.036 W/m/K. Estimated heat leakage from the laboratory room is 22 W for a 3 °C temperature difference between the room and the enclosure interior. Exterior dimensions of the enclosure are 1.5 m wide by 1.15 m high by 0.77 m deep.

The EE has two plenums, an air conditioner, and a main workspace. The workspace is 1 m wide by 0.66 m high by 0.66 m deep. Grilles form the ceiling and floor. The grilles are 6.35 mm aluminum plates perforated with 6.35 mm diameter holes on a staggered 12.7 mm pattern. The holes permit airflow through the workspace and provide a means of mounting equipment. Three of the walls of the workspace are solid and the fourth wall has a removable insulated door. A triple-glazed window in the door permits viewing the interior. The two plenums are located above and below the workspace. The air conditioner forms the left-hand portion of the EE. The plenum above the ceiling grille collects return air and is connected to the inlet of the air conditioner. The outlet of the air conditioner connects to the plenum below the floor grille. Four 2.94 m³/min fans move the air from the return air plenum into the air conditioner. The fans operate from regulated DC power to minimize speed variations. Each fan dissipates approximately 5 W. Removable insulated panels cover the air conditioner and plenums.

^b Dow Chemical Company Styrofoam®; Extruded polystyrene foam insulation board; R = 3.75 ft²h°F/Btu; (www.dow.com/styrofoam)

The temperature of the EE is controlled by a two stage Peltier air conditioner. The first stage contains two dual-element Peltier assemblies while the second stage has a single dual-element assembly. Each assembly consists of two commercial Peltier devices^c of nominal 50-watt capacity sandwiched between a substantial, finned aluminum heat sink and a water-cooled copper block. Each fan on the Peltier assemblies dissipates approximately 5 W. Baffles in the air conditioner improve the air mixing by adding turbulence. Temperature sensors between stages and at the outlet provide signals for regulation of the air temperature. Additional sensors monitor the temperature of the EE air at the ceiling and at the inlet to the air conditioner.

The water circuit for these Peltiers consists of a 114-liter vessel, a small circulating pump, and a fan and radiator assembly. The large external vessel serves as a thermal capacitor, reducing the effect of sudden changes in room temperature.

The capacity of the EE air conditioner is adequate for CC dissipation of about 20 W plus the other heat sources in the EE. The additional loading of the air conditioner comes from the flowmeter equipment, circulating fans, ohmic losses in the electrical circuits, Active Insulation (AI) heaters, EE light, and heat ingress from the laboratory room. The air conditioner maintains the EE at 24.5 °C for most experiments. The control system permits a smooth transition between cooling and heating, minimizing temperature lag and overshoot. The Peltier assemblies also provide enclosure heating when needed. The relative humidity in the EE is about 45% at 25 °C. Under these conditions, the dew point is approximately 15 °C. We have not observed condensation on the air conditioning cooling assemblies. Condensate drains are not used.

3.3. *Calorimetry Chamber (CC)*

The CC is a cubical chamber located within the EE. Each wall has an interior 6.35 mm aluminum panel, covered by two layers of 19 mm rigid polystyrene foam insulation. An additional 6.35 mm aluminum panel is attached to the outer surface of this insulation and a final layer of 19 mm rigid polystyrene foam insulation covers the entire assembly. Rigid PVC angle material holds the panels at the edges and provides a slight separation. This arrangement makes the panels thermally independent. The inner dimensions of the chamber are 25 cm by 25 cm by 25 cm. The outer dimensions of the chamber assembly are approximately 35 cm by 35 cm by 35 cm. The front of the CC is a gasketed and insulated hinged door with mitered edges that fit snugly with the adjacent sides of the chamber. The CC is attached to the bottom grille of the EE by four 14 cm long by 19 mm diameter phenolic stand-offs.

The walls of the CC form the Active Insulation (AI). Each outer aluminum panel has 16 series-connected 1 Ω resistors^d attached to its surface that act as heaters. An imbedded temperature sensor is located at the center of each outer panel. A corresponding sensor is located at the center of the adjacent inner panel. The heating resistors connect to the outputs of six independent feedback-loop controllers. The set point for each feedback loop is the temperature of the inner aluminum panel. With this arrangement, the output of each controller forces the temperature of each outer panel to match that of the corresponding inner panel. The term “Active Insulation” (AI) refers to this temperature-tracking technique. The technique produces near-adiabatic conditions. In other words, no heat transfer to or from the CC interior takes place through the chamber walls.

There are several components inside the CC. A liquid-air heat exchanger^e and circulating fan occupy the left side of the chamber. A regulated DC voltage operates the heat exchanger fan. A tachometer sensor within the fan permits monitoring of the fan speed by the system software. The fan speed varies slightly with chamber temperature as the air viscosity changes. At constant temperature, the nominal fan speed is 1600 RPM, with a one-sigma standard deviation of about 0.2 RPM. We avoid a variable power contribution to the calorimetry measurements by deliberately leaving the fan speed unregulated. Fan power dissipation remains close to 0.86

^c Melcor Corporation; Type CP 1.4-127-06L; 6 Ampere, 51.4 watts at $\Delta T = 0$; (www.melcor.com)

^d Caddock Electronics, Inc.; Type MP915; 1 ohm, 1%, MF, 15W, TO-126 (www.caddock.com)

^e Lytron Corporation; Model 6105 G1SB Copper Tube Heat Exchanger; (www.lytron.com)

watts during experimental runs. Between the heat exchanger and the open area where cells are located is the permanent calibration heater. Typically, a stand constructed of phenolic is attached to the bottom panel to hold the cell in the approximate center of the open space of the chamber and permit free circulation of air around it.

There are ports in the chamber walls for electrical connections, optical instruments and gas and liquid handling. Two ports are located on the bottom of the chamber to admit wiring for the heat exchanger fan, calibration resistors, cell power, AI panel heaters, and temperature sensors for the cell and AI panels.

Three small optical ports are located on the right side of the CC. One port is primarily used for a borescope to allow viewing of the cell. A matched port is located in the side of the EE allowing borescope access from the laboratory outside the enclosure. A small video camera optionally attaches to the borescope. The other two ports were designed for a laser or other device to illuminate a portion of the cell. A small phenolic tube in these ports, closed at the ends with microscope cover glasses, reduces heat transfer and provides a clear optical path.

In order to prevent dangerous pressures inside closed cells, MOAC has an automatic cell venting system. A 3 mm I.D. PVC tube connects the cell, through a liquid trap in the CC, to a capacitance manometer^f and solenoid relief valve outside of the EE. The manometer output is monitored and recorded by the main computer. Pressures outside of the range 700 Torr to 800 Torr trigger the opening of the solenoid valve. This valve is normally open which ensures that in the case of power failure, the valve stays open. A syringe or other volumetric device connected to the pressure line permits the determination of the total headspace volume as well as providing an indication that the cell is sealed.

Some experiments require periodic additions of fluid to the cell. A 1.6 mm I.D. TFE refill tube runs from the interior of the CC to the outside of the EE, where it can be connected to a syringe. The interior end of the refill tube connects to the cell when required, allowing it to be refilled during operation without opening the calorimeter. A retainer prevents displacement of the syringe plunger by the pressure in the cell.

3.4. Calorimetry Water Loop

Distilled water flows in a recirculating loop and serves as the medium for heat removal from the CC. Accurate power measurement depends upon a stable and accurately known flow rate. The use of a positive-displacement pump and a precision flowmeter produces excellent results. The entire calorimetry water loop is within the temperature-controlled environment of the EE.

The calorimetry water loop consists of a heat exchanger, three temperature regulators, a flowmeter, a circulating pump, a stirred reservoir, and three air traps. Water enters the CC and passes through the heat exchanger where it collects heat from the experiment. After leaving the CC, the water passes through an air trap and into the first-stage temperature regulator. The water then passes through the flowmeter and into a stirred reservoir. From there, the water is drawn through the second air trap into the pump and out into the third air trap. Finally, the water circulates into the second- and third- stage temperature regulators before entering the CC again.

Temperature sensors are located at the boundary of the CC in both the inlet and outlet lines. The temperature at each point is determined by averaging the readings of a pair of sensors. The inherent offset between the inlet and outlet sensor pairs was measured prior to their installation and is used in power calculations.

For regulation of the calorimetry water temperature, three single-element assemblies were constructed with a Peltier device sandwiched between two copper blocks. One copper block in each assembly is made with a labyrinthine water passage and fitted with copper inlet and outlet tubes for connection to the flow loop. The first-stage regulator is attached to the ceiling grille and thus delivers the bulk of the heat extracted from the CC directly to the EE air conditioner. The second-stage and third-stage regulators, which make only small changes in the water temperature have a larger copper block that serves as a heat sink and thermal capacitor to minimize sudden changes in the cooling or heating characteristics of the regulator. With the entire calorimetry water loop

^f MKS Instruments Inc.; Baratron® Capacitance Manometer; Model 222BHS-B-B-1000; (www.mksinst.com)

located within the controlled temperature of the EE, the water temperature is maintained close to the desired heat exchanger inlet temperature. This allows the second-stage and third-stage temperature regulators to run in a lightly loaded, near-idle state.

The water flow rate is measured by a mechanism consisting of a 100 ml cup secured to the platen of a digital balance^g. The cup fills with calorimetry water when a diverter valve is operated for a precisely timed period. The cup is weighed just before each filling to determine the tare. After filling and settling, the cup is again weighed to determine the gross weight accumulated during the timed fill period. When the weight has been measured, the cup is drained into a small dump pan from which the water returns to the reservoir. The calorimetry water stream is diverted to the cup only during a flow rate measurement. Otherwise, it bypasses the cup and flows directly to the reservoir. The cup dump valve is operated by a motor-and-lever mechanism that is arranged to remain clear of the cup during the taring and weighing portions of the flowmeter cycle. The digital balance is connected to the main computer through a serial communications port. The main computer software controls the flowmeter cycle by the use of a crystal-based counter-timer function, avoiding timing uncertainties associated with the computer operating system delays and the computer clock. Measurement time and related delays are set so that sufficient time is allowed for settling of disturbances caused by the filling and dumping of the flowmeter cup. A complete cycle of the flowmeter takes about 1.5 minutes. We typically observe one-sigma deviation in the measured flow rate of about 0.0005 gm/sec, which is 0.02% relative.

The positive-displacement pump is a modified commercial device^h. It has a ceramic piston that rotates and reciprocates in a ceramic cylinder. Displacement is adjusted by changing the angle between the pump head and its drive shaft. At 1800 RPM and the current angle setting, the mass flow rate is about 2.47 gm/s. The pump is located at the lowest point in the process loop. The manufacturer's seals were removed to reduce friction, which was found to be variable and to produce as much as one watt of heating of the pumped water. Absence of the seals has not caused leakage or permitted air ingress. The pump is driven by an AC synchronous motorⁱ that is mounted outside the EE to remove its significant heat load from the Peltier air conditioners. An extended shaft connects the motor to the circulating pump on the bottom grille of the enclosure. The motor is powered by a precision-frequency supply based on a 6-Megahertz quartz crystal standard.

The reservoir is a 3.8-liter plastic container of commercial distilled water located in the EE. A motor driven stirrer and the reservoir inlet and outlet connections mount on an aluminum cap that fits snugly on the top of the jug in place of the usual plastic cap. This arrangement permits rapid change of the reservoir and its contents. The inlet connection deposits the returning calorimetry water near the top of the reservoir. The outgoing calorimetry water comes from the bottom of the reservoir. A regulated DC source provides the power for the stirrer motor. A spare container of distilled water is stored in the EE for quick reservoir change without creating a water temperature disturbance.

Each air trap consists of an inverted polypropylene centrifuge tube with a stopper that holds inlet and outlet tubes. Entrained and dissolved air in the water rises to the conical upper end of the tube. The markings on the transparent tubes provide a convenient means of estimating the amount of trapped air. Most of the air is trapped in the tube immediately following the reservoir. The air traps prevent air from accumulating in the heat exchanger. A valve mounted on a tee just prior to the second-stage temperature regulator is used with a water-filled syringe to purge air from the system after maintenance.

^g Ohaus Corporation; Model Scout II; Digital Scale; 200 gm capacity, 0.01 gm readability, 0.01 gm repeatability, +/-0.01 gm linearity; (www.ohaus.com)

^h Fluid Metering Incorporated; Model RVH1CKC; (www.fmipump.com)

ⁱ Oriental Motor U.S.A. Corporation; Model 3SK10A-AULA; (www.orientalmotor.com)

3.5. Computer System and Software

Two desktop computers^j handle MOAC operation using Windows 2000 Professional and Labview 7 Graphical Environment Program^k as the basis for the calorimeter control program. The computers are designated as the auxiliary computer and the main computer.

An analog input board and an analog output board reside in the auxiliary computer. The analog input card receives signals from twenty-two thermistor temperature sensors. The analog output board provides the drive signals for eleven power operational amplifier modules. This card also provides six channels of digital on-off control for calorimeter functions

The auxiliary computer is responsible for the control of the AI panels, the second-stage and first-stage calorimetry water temperature regulators, the EE air conditioning system, as well as the measurement, display, and recording of the temperatures of the calorimetry water, the cooling air temperatures and the AI panels as well as the voltages of the Peltier devices and AI panel heaters. This software also includes on-off control of the calorimeter power supplies, the circulating pump, and the EE light.

The main computer is fitted with an analog input board, an analog output board, and a counter-timer board. The analog input card receives signals from fourteen thermistor temperature sensors and from eight voltage and current sensing circuits related to input power measurements. The crystal-based counter-timer function of the analog input card controls the flowmeter fill valve. The analog output board in the main computer provides drive signals for five power operational amplifier modules. It also provides three channels of digital off-on control of calorimeter functions. The counter-timer board^l in the main computer controls the monitoring, calculation, and display of the speeds of the heat exchanger fan and circulating pump motor. The use of the crystal oscillator on the counter-timer board avoids uncertainties of the computer clock and operating system timing. The serial interface port on the main computer is used with the ASCII data output of the flowmeter balance.

The main computer is responsible for control of the flowmeter and regulation of the heat exchanger inlet water temperature. It is also responsible for input and output power measurements, related data analysis and statistical calculations, as well as the measurement, display, recording, and statistical analysis of other operating parameters.

The software in both computers records the experimental data to disk files. Subsequent playback of these files permits detailed examination of events that have occurred during an experimental run.

All operation of MOAC is by means of the graphical programming environment. This software provides excellent display capability and relative ease of developing complex programs using ready-made modules. Particular use was made of the PID controller functions, the statistical functions, and the data display capability. The library of standard functions was augmented with custom-made modules and formula blocks.

A feature in the graphical environment software permits publication of the current screen displays on the Internet. System operators and experimenters have a separate password-protected program^m for remote control, logbook entry, and emergency shutdown.

^j Two system computers are used. Each has an ABIT motherboard, Athlon XP2600+ CPU, 500 Megabyte RAM, 80 GB Hard Drive, and LAN Interface.

^k National Instruments Corporation; (www.ni.com)

^l Measurement Computing Corporation; Model CIO-CTR05 Counter-Timer Board; (www.measurementcomputing.com)

^m UltraVNC Ltd. UK; Virtual Network Computing Software; (www.uvnc.com)

3.6. Video Camera System

A color video camera with zoom and pan-tilt functions is mounted in the laboratory to permit viewing of the calorimeter system, its computer screens, and its peripheral equipment. Audio monitoring is also available. The camera is publicly accessible and controllable via the Internet.

4. Measurement and Regulation

4.1. Temperature Measurement

Precise temperature measurement is essential to the operation of a calorimeter. We chose thermistor sensors because of their relatively high sensitivity, reproducibility, interchangeability, as well as small size and short time constant. The temperature sensors in MOAC are 10K Ω (at 25 °C) commercial thermistorsⁿ. These are negative temperature coefficient devices with a guaranteed interchangeability of 0.1 °C, and a stability specification of 0.011 °C aging per year at 75 °C. Observed stability in the calorimeter is considerably better, likely due to the low operating temperature, absence of physical stress, and avoidance of higher temperatures during handling and installation.

Nonlinearity of the thermistor temperature-resistance characteristic requires use of the Steinhart-Hart equation and its empirically derived coefficients to determine temperature^o. A voltage divider with the thermistor as the lower element and a ± 50 ppm/°C precision 10K Ω fixed resistor^p as the upper element provides the means of resistance measurement. A highly regulated 2.5 V DC voltage supplies the divider. The thermistor signal is very close to 1.25 V at 25 °C. The signal from the voltage divider tap is fed into an analog input on the computer. Use of a relatively low voltage across the sensors reduces self-heating. Thermistor dissipation is less than 0.0002 W. The software converts the non-linear thermistor voltage signal to temperature. The conversion requires accurate values for the voltage applied to the voltage divider and for the fixed resistance in each channel. These values were determined during fabrication of the individual dividers and of each regulated voltage source. Each fixed resistor was measured at 27 °C with a reliable instrument^q and its value entered into the software. Each voltage regulator output was measured to obtain its actual output voltage and its temperature coefficient. For the two voltage regulators used in the MOAC system, one has a temperature coefficient of -0.0035%/°C and the other has a coefficient of +0.0056%/°C. Both values are consistent with the manufacturer's specifications.

Two precision voltage regulator^r circuit board assemblies are mounted in the temperature-controlled portion of the EE. Each assembly accommodates up to 24 sensors. Some of the unused channels are fitted with fixed resistors instead of thermistors, to permit monitoring of the condition of the voltage regulator and to provide an indication of the noise floor of the temperature measuring system. Care has been taken with the sensor wiring to

ⁿ Betatherm Corporation; Type 10K3A1A Thermistor; (www.betatherm.com)

^o I.S. Steinhart & S.R. Hart in "Deep Sea Research" Vol. 15, p. 497 (1968).
See also: [www.http://www.betatherm.com/stein.htm](http://www.betatherm.com/stein.htm) for further information specific to Betatherm thermistors.
The general form of the equation is: $1/T_K = A + B(\ln(R)) + C(\ln(R))^3$.
For the Betatherm 10K3 thermistor, $A = 1.129241 \times 10^{-3}$; $B = 2.341077 \times 10^{-4}$; and $C = 8.775468 \times 10^{-8}$, for calibration points at 0°C, 25°C and 70°C.

^p Vishay; BC Components; Type BC207C-F; 1%, 0.4 W, Metal Film;
(www.vishay.com/company/brands/bccomponents)

^q Keithley Instruments Inc.; Model 2000 Digital Multimeter; 6.5 digits; (www.keithley.com)

^r National Semiconductor Corporation; Type LM723 Voltage Regulator; (www.national.com)

avoid ground loops and noise pickup. The sensor signals are connected to differential inputs of the analog boards in the computers.

4.2. Temperature Regulation

Temperature regulation is of critical importance in the design of a precision calorimeter. Heating and cooling capability is necessary for the EE and for the regulation of the calorimetry water temperature. Proportional instead of “on-off” control is employed.

A bipolar drive signal is fed to each Peltier element to provide a smooth transition between cooling and heating. Each element is driven by its own power operational amplifier^s assembly. These modules have a voltage gain of 2.4, originally chosen so that an input signal of 0-5 V would produce an output signal of 0-12 V for the Peltier element. The input signal range was later changed to 0-6 V to permit the application of more than 12 volts to the Peltier, a change necessitated to overcome circuit losses caused by the resistance of the wiring. Each assembly uses Peltier elements of nominal 50-watt capacity.

The signals from the temperature control sensors are fed into the analog input boards^t in the system computers. The software uses each signal as the process variable input of a software proportional-integral-derivative (PID) controller with a programmable set point. The output of the PID controls the signal generated by the computer’s analog output board^u. The analog output drives the input of the power operational amplifier module. A closed feedback loop is created by this arrangement. The thermal time constants of the various temperature regulators differ, making it necessary to tune the individual PID controller. Controller tuning was accomplished empirically by observing the response of each regulator to step changes in its set point or load.

The closed-loop regulation scheme achieves exceptionally close control of temperature. We typically observe one-sigma deviations of 0.001 °C for the temperature of the water leaving the second-stage regulator and 0.0007 °C for the temperature of the water leaving the third-stage temperature regulator. For the EE air conditioner, we typically observe one-sigma deviations of 0.0015 °C for the temperature at the outlet. For the active insulation, temperature differences between the inner and outer panels of the AI are about 0.0002 °C when equilibrated.

MOAC uses twelve power operational amplifier modules to control the six AI panels, the three EE air conditioner Peltier assemblies, and the three water temperature regulators. Power is obtained from linear power supplies to avoid noise problems that can arise from switching-type power supplies. Six linear supplies are used for the AI and Peltier assembly power sources. A seventh linear power supply is used with the operational amplifier modules that control the power to the calibration resistors and the cell.

4.3. CC Input Power

Operational amplifier modules are used for control of the cell and for control of two calibration resistors. These modules are in closed feedback loops similar to those used with the temperature regulation channels. Input power is determined by the input voltages and currents of the devices within the CC:

$$P_{in} = V_{in} \cdot I_{in} \quad (1)$$

where V_{in} is the voltage at the boundary of the CC, and I_{in} is the current through the device. In the case of multiple devices, the total power is the sum of the individual device dissipations.

^s National Semiconductor Corporation; Type LM12CL 80 Watt Operational Amplifier; (www.national.com)

^t Measurement Computing Corporation; Model PCI-DAS6033 16 Bit, 64 Channel Analog Input Board; (www.measurementcomputing.com)

^u Measurement Computing Corporation; Model PCI-DAC6703 16 Bit, 16 Channel Analog Output Board; (www.measurementcomputing.com)

A four wire sensing configuration is used for voltage measurements. The sensing connection is made to the terminal block points to which the load device wires are connected. The measurement reflects only the voltage at that point and a correction must be applied to compensate for ohmic losses, even in the relatively short wires from the terminal block to the boundary of the CC. The voltage sensing wires are connected to 2:1 resistive dividers mounted on the terminal block and run to the differential inputs of analog input boards in the system computers.

The voltage divider arrangement is necessary because some experiments require application of voltages beyond the 10 V limit of the analog input channels. The voltage dividers are constructed with ± 50 ppm/ $^{\circ}\text{C}$, 10K Ω precision metal film fixed resistors^v. The resistors used in each of the dividers were measured with a reliable instrument and paired. The divider ratio was calculated and entered into the voltage measurement portion of the software.

Current is measured as a voltage drop across a resistor in series with each device. For each current measurement, a ± 50 ppm/ $^{\circ}\text{C}$ precision fixed 1 Ω power resistor^w is used, except for the cell current where a 0.5-ohm resistor is used to accommodate higher device currents. Voltage sensing wires are connected to the terminals of each current sensing resistor and run to the differential inputs of analog input boards in the system computers. This is also a four-wire configuration. Insertion of the series current sensing resistor results in a voltage drop between the terminal block and the CC boundary, which is corrected for in the software. Measured values of the sensing resistors are used in the current measurement portion of the system software. The current sensing resistors are mounted to the floor grille of the EE for heat dissipation and temperature stability.

The resistances of the connecting wires between the measurement points and the load points were determined by measuring the length of the each pair of wires and calculating their resistance from the known 0.004016 Ω per foot resistance of the 16 gauge copper wire. The wire resistances are entered into the device power calculations in the software.

Wires that connect the load devices to the terminal blocks dissipate a small amount of power. Inside the CC, this power appears as heat to be absorbed in the heat exchanger, and is not distinguished from the dissipation of the load devices. Outside the CC, the heat is lost to the EE environment and does not enter into the power calculations.

In addition to the measurements of the actual resistance values used in the power measuring circuits, the voltages and currents were measured with independent instruments and found to agree well with the corresponding values measured by the analog input boards and associated software.

4.4. CC Output Power

The rise in water temperature across the heat exchanger and the mass flow of the water are used to determine the power dissipated in the CC:

$$P_{\text{flow}} = \Delta T \cdot \Gamma \cdot c \quad (2)$$

where: $\Delta T = T_{\text{out}} - T_{\text{in}} + \text{Sensor Offset}$; Γ = the mean flow rate in gm/s; and $c = 4.1796$ J/gm- $^{\circ}\text{C}$ at 25 $^{\circ}\text{C}$. The values T_{out} and T_{in} are the averages of the temperatures indicated by the individual sensors in each dual-thermistor sensor assembly at the boundaries of the CC. With no heat source in the chamber, the difference between the outlet and inlet water temperatures should be zero. Small differences in the sensors create an offset between the inlet and outlet temperature indications at zero power that must be taken into account in the calculation of ΔT .

For calibration, accurately known electrical power levels are applied to any or all of several devices inside the CC. First, the permanent calibration heater, R1, is always employed so that the calibration may be checked at a later date no matter what changes have been made to the cell. Second, a standard electrolysis cell, made

^v Panasonic Type ERO-S2PHF1002; 1%, 0.25 W, Metal Film; (www.panasonic.com/industrial/components)

^w Caddock Electronics, Inc.; Type MP930; 1%, MF, 30W. TO-220; (www.caddock.com)

with Pt-Pt electrodes and H₂O-H₂SO₄ electrolyte with Pt catalyst recombiner in the headspace, is operated to provide a heat source that closely mimics a real cold fusion cell. Third, another calibration heater, R2, is immersed in the electrolyte of the cell to provide yet another heat distribution for calibration purposes. These three heat sources are operated singly and in combination at different power levels for extended periods to acquire the calibration data. The readings are used in a statistical regression analysis to obtain the slope, intercept, and quality of fit of the calibration curve. Coefficients **a** (intercept: watts) and **b** (slope: dimensionless) are obtained. The coefficients are then used in the calorimeter power equation:

$$P_{\text{flow(cal)}} = a + b \cdot P_{\text{flow}} + \text{wire loss} \quad (3)$$

The term *wire loss* is the effect of the thermal conductivity of the copper wires entering the CC through the bottom ports. Each bundle of wires has temperature sensors imbedded where the wires pass through the inner and outer aluminum panels of the CC. The wire cross-sectional area, length, thermal conductivity, and temperature difference between the inner and outer surfaces are used to calculate the wire loss correction term. The thermal conductivity of the vinyl insulation on the wires was ignored because it is only about 10⁻⁴ of the conductivity of the copper conductors. When 10 W is dissipated in the chamber, the wire loss is typically about 60 mW.

5. Performance

The primary measure of MOAC's performance is its overall measurement accuracy. When recently calibrated, MOAC can achieve the original design goal of +/- 0.1% relative accuracy. Table 1 shows a typical calibration regression result which provides the coefficients **a** and **b** for equation 3.

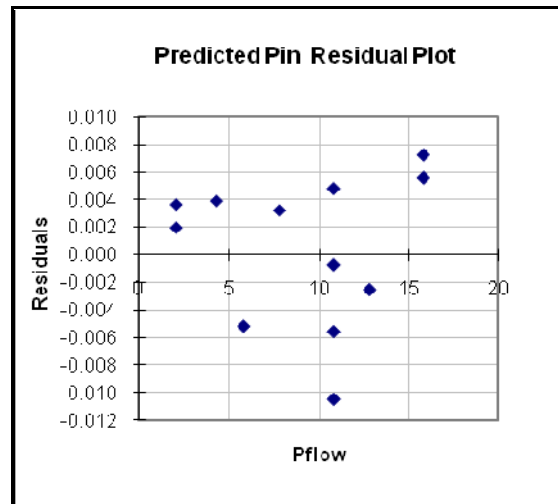
Table 1. Calibration Regression

<i>Regression Statistics</i>		5R1+5R2+5E	15.8437	0.0056
Multiple R	0.999999281	12E	12.8519	-0.0025
R Square	0.999998562	10E	10.8572	-0.0062
Adjusted R Square	0.999998431			
Standard Error	0.005744603			
Observations	13			

	<i>Coefficients</i>	<i>Standard Error</i>
a	0.010942798	0.00372184
b	1.000451508	0.000361737

RESIDUAL OUTPUT

<i>Heat Source</i>	<i>Predicted Pin</i>	<i>Residuals</i>
10R1	10.8512	-0.0007
10R2	10.8603	-0.0105
10E	10.8561	-0.0056
5R1	5.8569	-0.0052
1.25E	2.1028	0.0020
1.25R1	2.1015	0.0037
3.5R1	4.3506	0.0039
7R1	7.8507	0.0032
10R1	10.8482	0.0048
10R1+5R2	15.8447	0.0073



Note how close the value of **b** is to unity. This demonstrates the fundamental nature of this approach to calorimetry and also shows that MOAC's thermal design is successful in removing heat from the chamber only via the flowing water.

Another important aspect of performance is specimen versatility. MOAC excels in this area by producing precisely the same reading on a wide variety of heat sources. The size, shape, temperature, and location within the chamber have very little effect on the measurement.

In Table 1 above, note how closely the various heat sources (R1, R2, and E - electrolysis power) fit the calibration line. This is a clear demonstration of MOAC's excellent specimen versatility. We also conducted a location study in which a calibration heater was operated at 15 watts at several different locations within the CC. For all the reasonable locations, the difference between electrical input power and heat output power was 12 mW or less (i.e. within 0.1% relative). When the calibration heater was placed in one of the extreme corners of the chamber, the heat output power read 25 mW lower than the electrical input power (i.e. a 0.2% error).

5.1. Errors

MOAC exhibits both random and systematic errors. The random errors appear to be a combination of electrical noise and digital granularity in the temperature measurements. This conclusion is supported by the fact that fixed precision resistors located within the environmental enclosure report about the same jitter as the thermistors. Even with 100-reading averages comprising each observation, these errors produce a jitter in the temperature signals of about ± 0.0005 °C. Given MOAC's 10 W/°C sensitivity and the fact that inlet and outlet water temperatures are measured independently, this jitter corresponds to almost ± 10 mW in the heat output power signal. Fortunately, MOAC's thermal time constant is about one hour so it is permissible to apply additional averaging to the signals to reduce this jitter to negligible levels.

The systematic errors are more complex. When MOAC was first commissioned in the summer of 2004, it readily achieved 1% relative accuracy. However, numerous systematic errors prevented it from approaching the design goal of 0.1% accuracy. It took nearly 2 years of intensive testing and evaluation to find and eliminate these errors.

For the first few months of operation we observed mysterious perturbations in the heat output power reading. Usually the reading would slowly recover to the value before the disturbance. We finally determined that these perturbations were due to the sudden expulsion of an air bubble in the liquid-air heat exchanger in the CC. When the bubble departed, the wetted area of the heat exchanger was suddenly increased, which increased its efficiency and thus cooled the contents of the chamber slightly. We solved this problem by installing three air traps at strategic locations in the calorimetry water loop. The trap located just after the water is drawn from the stirred reservoir collects the most air and must be emptied every two or three months.

Another problem that caused noticeable short-term drift was instability in the water flow rate. We initially constructed MOAC with a pump system from FMI that was advertised to provide a highly stable flow rate. Once we identified pump speed variations as the problem we abandoned the FMI controller and tried a custom closed-loop speed control that employed a digital tachometer. That worked better but the brushes in the DC pump motor caused undesirable speed perturbations. After trying another type of DC motor with similar results we abandoned DC motors altogether and installed a synchronous AC motor powered by the 120VAC 60Hz mains. Small line frequency variations were clearly visible in the measured flow rate. Finally we conquered the flow rate stability problem by constructing a crystal-based 60Hz power supply for the synchronous motor. The result is a flow rate whose stability is typically $\pm 0.02\%$ relative.

For the first 6 months of operation, MOAC required a **b** calibration coefficient of approximately 1.01. In other words, we were losing 1% of the heat from the chamber. We tracked this loss down to the power and signal wires passing through the walls of the chamber. We initially thought that the active insulation system would eliminate losses in these wires because the temperature difference across the walls is forced to be zero. However, our wire bundles were not adequately thermally clamped at each wall so ambient air temperatures were having an unexpected influence. We solved this problem by instrumenting the wire bundles with temperature probes located at each wall of the CC. The measured temperature difference from these probes is

used to calculate the wire loss term used in equation 3. After this correction was implemented, the **b** coefficient typically comes out between 0.999 and 1.001; in other words, within 0.1% of unity.

A number of other issues have been identified and addressed over MOAC's four-year operating history. For example, we have struggled to find a suitable gasket for the calorimetry chamber door. Several designs were tried and some of them caused noticeable heat leaks. It must be remembered that a 0.5% loss is easily noticeable in a calorimeter that is expected to achieve 0.1% accuracy.

At the time of this writing, MOAC is quite reliable and readily achieves 0.1% accuracy when recently calibrated. The largest remaining source of error is the drift exhibited by the thermistors used for the critical inlet and outlet water temperature measurements. The observed drift is usually quite slow and is only a fraction of the manufacturer's specification. That is, the thermistors are performing significantly better than the manufacturer's guarantee but we can still see their drift. Because of this drift, MOAC typically requires recalibration, usually only a change in the **a** term, once every month or two.

6. Interesting Results

One of the primary reasons we constructed MOAC was to verify the excess heat effect in the laser-stimulated cold fusion cells of Dennis Letts. In Letts' laboratory, his cells often exhibit the Letts Effect, a sudden rise in electrolyte temperature in response to illuminating the Pd cathode with only ~20 mW of red laser light. According to isoperibolic calorimetry, this electrolyte temperature rise corresponds to an increase in heat output of 250-500 mW. However, isoperibolic calorimetry is generally not as reliable as flow calorimetry. Isoperibolic calorimetry is critically dependent upon the thermal coupling between the electrolyte and the surround air. This coupling is affected by parameters that are not necessarily stable. Examples include the convection current patterns in the electrolyte, circulation patterns in the surrounding air, bubbles adhering to the cell walls, and deposits of other material on the cell walls.

MOAC was specifically designed to permit operation of the Letts cell with both isoperibolic and flow calorimetry measurements occurring simultaneously. The observation of essentially the same excess heat signal in both measurements would verify that the Letts Effect was real excess heat.

Over the past four years Letts has run a number of cells in MOAC but none have produced a robust example of the Letts Effect. Because of this frustrating situation, we have not been able to use MOAC to determine whether the Letts Effect represents real excess heat or not.

However, we have observed some significant differences between isoperibolic and flow calorimetry results that deserve attention. Figure 5 shows MOAC's main computer screen during a run with a Letts cell. No lasers were used in this experiment. The plots depict an eight-hour period during which the electrical input power to the cell was constant at 8 W. The uppermost plot shows the isoperibolic calorimetry results. The vertical scale is 0.2 watts/div. The blue line is the electrical input power and the orange line is the heat output power as computed from the temperature difference between the electrolyte and the air around the cell inside the CC. Note the sharp increase that occurs around 0700. The heat output power, which was closely matched with the electrical input power, rises to a value about 600 mW greater. This is typical of the sudden rise that occurs in the Letts Effect but, in this case, there was no laser stimulation of the cathode. This event was spontaneous and, from the isoperibolic data alone, looked exactly like the sudden onset of 600 mW of excess heat.

The next plot down shows the flow calorimetry results. The vertical scale is 0.02 W/div. Again the blue line is the electrical input power but now it is about 0.85 W higher because it includes the power to the heat exchanger fan. The red line is the heat output power from the flow calorimetry. Instead of rising like the isoperibolic result, it dips and then returns to its original value. There is no sign of excess heat, especially not 600 mW, which would have driven the red line off the scale.

The middle plot shows the two electrolyte temperature probes (red and brown traces), which behaved similarly; cell pressure (cyan), which rose slightly during the event; and cell resistance, which dropped slightly. The next-to-bottom plot shows the flow rate (green) and inlet water temperature (black), both of which were very steady at all times. The bottom plot shows room temperature (pink) and the heat exchanger fan speed.

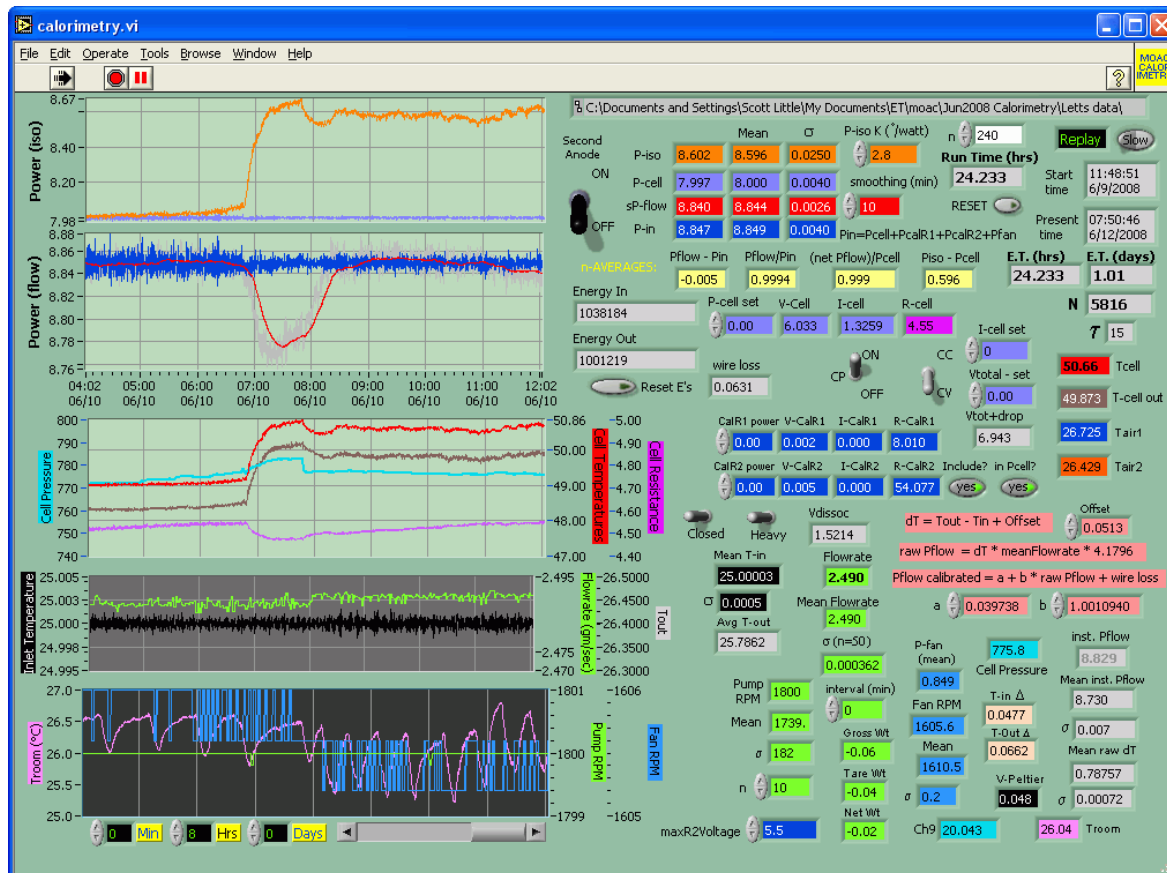


Figure 5. Letts Event

Unfortunately, none of these supporting data help us understand *why* the cell behaved as it did. But the top two plots are sufficient to understand *what* happened. This event was caused by a relatively sudden decrease in the thermal coupling coefficient between the electrolyte and the surrounding air. As the change occurred, electrolyte temperature necessarily rose to reestablish dynamic equilibrium. Because electrolyte temperature was rising, the internal energy of the electrolyte was increasing. Since the input power was constant at all times, Conservation of Energy required the heat output power to decrease accordingly, hence the behavior of the flow calorimetry data. This example clearly demonstrates the value of simultaneous calorimetric measurement by independent methods.

6.1. Simulated Excess Heat

To date, our operating experience with MOAC has been singularly devoid of opportunity to observe real excess heat signals. However, using R2, the calibration heater immersed in the electrolyte of our standard calibration cell, we can simulate an excess heat signal to see how MOAC responds. Figure 6 shows both the isoperibolic and flow calorimetry results for a 24-hour period during which our standard cell was operated at 10 W of electrolysis power.

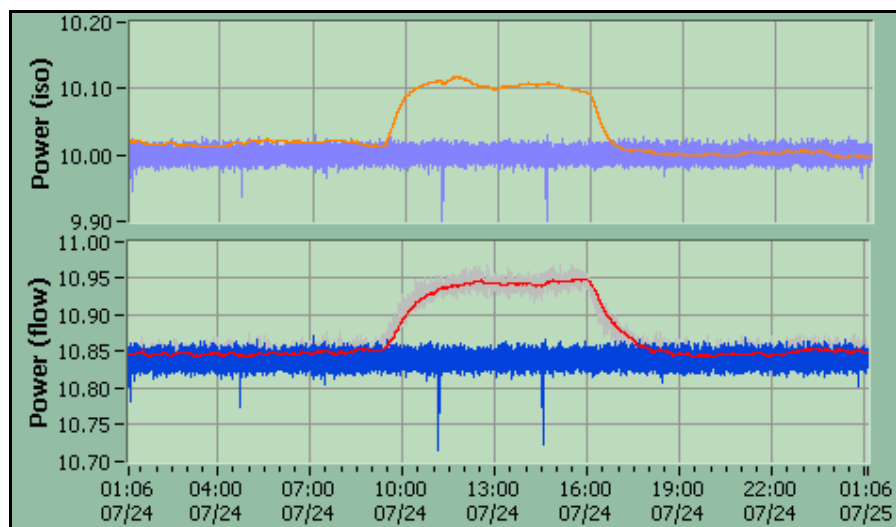


Figure 6. Simulated Excess Heat

At about 0900, a voltage was applied to R2 that caused the dissipation of an additional 100 mW in the electrolyte. To make this signal look like excess heat, the software was configured so that this power was not included in the plotted value of the electrical input power. As you can see, both the isoperibolic and flow traces rise up 100 mW above the electrical input power. At about 1600, the simulated excess heat signal was turned off. Clearly MOAC is capable of quantifying excess heat signals of this magnitude.